Hindawi
Wireless Communications and Mobile Computing
Volume 2022, Article ID 1858865, 12 pages
https://doi.org/10.1155/2022/1858865

Research Article

Direction-of-Arrival Estimation Method for Principal Singular Vectors Based on Multiple Toeplitz Matrices

Yaofeng Tang,[1,2] **Kuangang Fan**,[2,3] **Shuang Lei**,[2,3] **and Junfeng Cui**[4]

[1]*School of Mechanical and Electrical Engineering, Jiangxi University of Science and Technology, Ganzhou, Jiangxi 341000, China*
[2]*Key Laboratory of Magnetic Levitation Technology in Jiangxi Province, Ganzhou, Jiangxi 341000, China*
[3]*School of Electrical Engineering and Automation, Jiangxi University of Science and Technology, Ganzhou, Jiangxi 341000, China*
[4]*China Railway Signal & Communication Research & Design Institute Group Company Limited, Beijing 100070, China*

Correspondence should be addressed to Kuangang Fan; kuangangfriend@163.com

Received 16 May 2022; Revised 22 June 2022; Accepted 23 June 2022; Published 8 July 2022

Academic Editor: Fawad Zaman

A principal singular vector based on multiple Toeplitz matrices is proposed to solve the accuracy problem of direction-of-arrival (DOA) estimation for coherent signals. First, the data matrix received by uniform linear array (ULA) is transformed into a Toeplitz matrix. An equivalent covariance matrix is obtained by square weighted summation method using the Toeplitz matrix. Then, a polynomial containing DOA information is constructed because the signal space and the steering matrix have the same column space; the Toeplitz matrix is built using polynomial coefficients. The problem is transformed into solving linear equations by establishing the relationship between the Toeplitz matrix and the signal subspace. Furthermore, the weighted least square method is used to obtain multiple candidates for linear equations. Finally, the maximum likelihood (ML) rule is used to select source signal candidates from multiple candidates. In comparison with currently known algorithm, the proposed algorithm has the characteristics of high estimation accuracy, low-complexity, and strong anti-interference ability and resolution. Even when the signal-to-noise ratio (*SNR*) is low, the snapshot number is small, and multiple signals exist; this method can still provide good estimation performance and resolution, which is more than 90% in most cases. Simulation experiments verify the superiority of the algorithm.

1. Introduction

Array signal processing is a crucial research issue in signal processing and has been extensively used in radar [1, 2], sensor [3, 4], remote sensing [5–7], target detection [8, 9], and wireless communication [10–12].

As one of the most important research contents in array signal processing, direction-of-arrival (DOA) estimation has been the focus of scholars for decades. Scholars have put forward many excellent algorithms. Among them, DOA algorithm based on subspace is the most representative method in DOA estimation, including multiple signal classification (MUSIC) [13], estimation of signal parameters via rotational invariance techniques (ESPRIT) [14], and its variants [15–20]. MUSIC replaces data matrix by constructing sampling covariance matrix and then obtains DOA by spectral peak search, which has high signal source detection resolution. However, due to coherent signals, the performance of the algorithm degrades and DOA cannot be accurately estimated. ESPRIT algorithm uses the rotation invariance between signal subspaces caused by sensor arrays with translational invariance structure; it is used to obtain high-resolution DOA information. Similar to the MUSIC algorithm, the detection accuracy of DOA decreases seriously in the face of coherent signal detection.

Many techniques and algorithms for processing coherent signals, such as forward-only spatial smoothing (FOSS) [21] and forward/backward spatial smoothing (FBSS) [22], have been proposed by scholars to process coherent signals. These methods divide the total array into several subarrays and then use the average value of the subarray covariance matrix to solve the coherent signal direction finding. However, the disadvantage of these methods is that they reduce the array aperture, resulting in reduced resolution of closely spaced

arrivals. In addition, signal subspace fitting (SSF) [23] and maximum likelihood (ML) [24–26] can solve the coherent signal by reducing the multidimensional problem to the 1D problem, without the need for feature decomposition in the process; it is insensitive to the coherence between signals. However, the number of signals greatly influences the estimation accuracy of the algorithm, and more signals indicate greater influence.

Recently, DOA algorithm based on polynomial solution, such as the method of direction estimation (MODE) [27, 28], the enhanced principal-singular-vector utilization for modal analysis (EPUMA) [29], and its variants [30–33], has received remarkable attention from scholars. MODE is similar to ML, but it can process coherent signals without complex computation and has no convergence problems. EPUMA is a low-complexity algorithm; it generates $(P + K)$ DOA candidates for K sources and then selects K to obtain coherent signal DOA information. Scholars have obtained good results by using these algorithms to solve coherent signals. However, in the low *SNR* and small snapshot number, they cannot accurately estimate, because the algorithm cannot accurately obtain sufficient signal information. If the source signal is highly correlated, then this situation will be exacerbated.

In addition, scholars have also proposed other excellent DOA algorithms [34–40]. In [34], a direction-of-arrival estimation algorithm based on low-rank reconstruction of the Toeplitz covariance matrix is proposed by scholars. In order to fully utilize the underlying received information in the presence of missing elements in the difference coarray, interpolation is performed and a dual variable rank minimization problem is formulated. The scholars recast the problem as a multiconvex form and developed an alternative optimization mechanism to solve the problem through cyclic iterations. In [35], a modified scheme based on forward and backward partial Toeplitz matrices reconstruction named as FB-PTMR is proposed. The scholars exploited half rows of the sample covariance matrix (SCM) to reconstruct the data matrix to overcome the performance deterioration of ESPRIT-like algorithm. In [36], the scholars used the existing decoherence algorithm, where the sample covariance matrix of each row is formed into a full-rank Toeplitz matrix to achieve decoherence, and then a new cost function to obtain DOA via a 1-D search. The advantage of the algorithm is that it does not require to know the source number information. In [37], aiming at the fact that conventional algorithms based on the convex relaxation is computationally expensive, the scholars proposed a nonconvex accelerated structured alternating projection-based direction-of-arrival estimation approach without solving semidefinite programming. In [38], the scholars proposed a new real-valued transformation for DOA estimation with arbitrary linear arrays by exploiting the virtual steering of linear arrays, which achieve a better performance in terms of both estimation accuracy and computational complexity. In [39], a DOA algorithm based on correlation matrix rearrangement is proposed. The algorithm can effectively deal with coherent signals in both 1D and 2D. In [40], an algorithm called MTOEP is proposed. MTOEP uses Toeplitz matrix and the observation data of each sensor to calculate a set of correlation matrices and then sums the square weighted of these correlation matrices to form the full-rank equivalent data covariance matrix. However, when multiple related signals and independent signals coexist, the error of this algorithm increases; a higher degree of correlation that exists between signals indicates greater error.

We propose a principal singular vector algorithm based on multi-Toeplitz matrix to eliminate the weakness of the existing algorithm. The proposed algorithm constructs a new covariance matrix and polynomial containing signal information by using the characteristic matrix, where the received data moments and signal space have the same column space as the steering matrix. The estimation problem is transformed into a linear equation problem, and the proposed algorithm has a better resolution effect. This algorithm combines the advantages of Toeplitz matrix and polynomial solution to obtain a high precision estimation algorithm without noise processing and auxiliary matrix. Subsequent experiments prove that the proposed algorithm can process multiple signals with low *SNR*, or the snapshot number is small and still has good performance.

This paper is organized as follows: we introduce the proposed algorithm in Section 2. In Section 3, we perform a series of simulation experiments. Finally, we summarize the study.

1.1. Notations. Superscripts $(\cdot)^{\dagger}$, $(\cdot)^{T}$, $(\cdot)^{H}$, $(\cdot)^{-1}$, and $(\cdot)^{*}$ represent the matrix pseudoinverse, matrix transpose, matrix conjugate transpose, matrix inversion, conjugate, and traces of matrix, respectively. The operator diag $\{\cdot\}$, E$\{\cdot\}$, vec$\{\cdot\}$, and $\otimes$ indicate diagonalization, expectation, vectorization, and Kronecker product, respectively. I_M and $0_{M\times N}$ denote $M \times M$ identity matrix and $M \times N$ zero matrix, respectively.

2. Proposed Algorithm

2.1. Signal Model. The uniform linear array (ULA) consists of $2\,\mathrm{M}+1$ isotropic sensors, each spaced $d = \lambda/2$ apart, assuming that K narrow band signals impinge on the array in the distance. The received signal is expressed as follows:

$$x(t) = As(t) + n(t), t = -M, \cdots, M, \tag{1}$$

where $A = [\mathbf{a}(\theta_1) \cdots \mathbf{a}(\theta_K)]$ is the steering matrix, $s(t) = [s_1(t) \cdots s_K(t)]^T$ denotes the $K \times 1$ source signal vector, $n(t)$ is Gaussian white noise vector with zero mean and variance σ_n^2, and snapshot number is N. The incident angle of the kth signal is θ_K, and the steering vector due to the kth source is expressed as follows:

$$\mathbf{a}(\theta_k) = \left[e^{-j2\pi M \sin(\theta_k)d/\lambda}, \cdots, 1, \cdots, e^{j2\pi M \sin(\theta_k)d/\lambda}\right]^T, \tag{2}$$

where λ is the carrier wavelength.

2.2. Equivalent Covariance Matrix Is Constructed Based on Toeplitz Matrix of Data Matrix. We use data matrix $x(t)$

to construct $(M+1)\times(M+1)$ Toeplitz matrix, whose expression is as follows:

$$\begin{aligned} R_X(t) &= \begin{bmatrix} x_0(t) & x_1(t) & \cdots & x_M(t) \\ x_{-1}(t) & x_0(t) & \cdots & x_{M-1}(t) \\ \vdots & \vdots & \ddots & \vdots \\ x_{-M}(t) & x_{-M+1}(t) & \cdots & x_0(t) \end{bmatrix} \\ &= R_{As}(t) + R_N(t), \end{aligned} \tag{3}$$

where

$$\begin{aligned} R_{As}(t) &= \begin{bmatrix} y_0(t) & y_1(t) & \cdots & y_M(t) \\ y_{-1}(t) & y_0(t) & \cdots & y_{M-1}(t) \\ \vdots & \vdots & \ddots & \vdots \\ y_{-M}(t) & y_{-M+1}(t) & \cdots & y_0(t) \end{bmatrix}, \\ R_N(t) &= \begin{bmatrix} n_0(t) & n_1(t) & \cdots & n_M(t) \\ n_{-1}(t) & n_0(t) & \cdots & n_{M-1}(t) \\ \vdots & \vdots & \ddots & \vdots \\ n_{-M}(t) & n_{-M+1}(t) & \cdots & n_0(t) \end{bmatrix}, \end{aligned} \tag{4}$$

are the $(M+1)\times(M+1)$ Toeplitz matrix constructed by the $As(t)$ and the noise vector $n(t)$, respectively. Therefore, we can obtain the correlation matrix between Rxi and the ith isotropic sensor output $x_i(t)$, as follows:

$$\begin{aligned} R_{Xi} &= \mathrm{E}[R_X(t)x_i^*(t)] = \mathrm{E}[R_{AS}(t)y_i^*(t)] + \mathrm{E}[R_N(t)n_i^*(t)] \\ &= R_{Asi} + \sigma_n^2\tilde{I}_{(M+1),i}, \end{aligned} \tag{5}$$

where $\tilde{I}_{(M+1),i}$ is an $(M+1)\times(M+1)$ matrix whose elements are zero, except the ith diagonal, which is unity element. We fully use Rxi information to avoid the decrease in the estimation accuracy caused by noise suppression and array output covariance matrix. The advantage of this approach is that the noise term is diagonalized to improve the estimation accuracy without the need for denoising. Then, we have the following:

$$\begin{aligned} \tilde{R} &= \sum_{i=-M}^{M} R_{Yi}R_{Yi}^H \\ &= \sum_{i=-M}^{M}\left[\left(R_{Xi} + \sigma_n^2\tilde{I}_{(M+1),i}\right)\left(R_{Xi} + \sigma_n^2\tilde{I}_{(M+1),i}\right)^H\right] \\ &= \sum_{i=-M}^{M} R_{Xi}R_{Xi}^H + \sum_{i=-M}^{M} R_{Xi}\sigma_n^2\tilde{I}_{(M+1),i}^H + \sum_{i=-M}^{M}\sigma_n^2\tilde{I}_{(M+1),i}R_{Xi}^H \\ &\quad + \sum_{i=-M}^{M}\sigma_n^4\tilde{I}_{(M+1),i}\tilde{I}_{(M+1),i}^H. \end{aligned} \tag{6}$$

According to formula (6), an equivalent covariance matrix can be obtained. In addition, to further improve performance, FBSS technology was used to further optimize the obtained equivalent R, which is expressed as follows:

$$R = \tilde{R} + J\tilde{R}^*J, \tag{7}$$

where J is a $(M+1)\times(M+1)$ matrix with antidiagonal, and the other element is zero. Then, singular value decomposition of R is obtained as follows:

$$\hat{R} = \hat{U}_s\hat{\Lambda}_s\hat{U}_s^H + \hat{U}_n\hat{\Lambda}_n\hat{U}_n^H, \tag{8}$$

where $\hat{R}$, $\hat{U}_s$, $\hat{U}_n$, $\hat{\Lambda}_s$, and $\hat{\Lambda}_n$ represent the estimated values of R, U_s, U_n, Λ_s, and Λ_n; Λ_s contains the signal eigenvalues, and Λ_n contains the noise eigenvalues.

2.3. Toeplitz Matrix Containing DOA Information Is Constructed. U_s and A have the same column space, according to linear prediction (LP) theory; thus, each column of U_s is a sum of P sinusoids. From [41], we obtain the following:

$$z_k^P + \sum_{i=1}^{P} r_i z_k^{P-i} = 0, \tag{9}$$

where $z_k = e^{j2\pi \sin(\theta_k)d/\lambda}$, $k = 1, \cdots, K$, and r_i represents the LP coefficients. According to LP coefficients, Toeplitz matrix $B(r)$ consists of polynomial formula (9) coefficients containing signal information, as follows:

$$\begin{aligned} B(r) &= Toeplitz\left(\left[r_K 0_{M-P-1}^T\right]^T, \left[r_K \cdots r_1 1 0_{M-P-1}^T\right]\right) \\ &= \begin{bmatrix} r_K & r_{K-1} & \cdots & r_0 & 0 & 0 & 0 \\ 0 & r_K & r_{K-1} & \cdots & r_0 & 0 & 0 \\ & \ddots & \ddots & \ddots & \ddots & \ddots & \\ 0 & 0 & 0 & r_K & r_{K-1} & \cdots & r_0 \end{bmatrix}^{\mathrm{H}}. \end{aligned} \tag{10}$$

2.4. Multiple DOA Candidates Were Obtained by Solving Linear Equations. The matrix form of formula (9) is as follows:

$$e_k = F_k r - g_k = 0_{M-P} \tag{11}$$

where

$$F_k = \begin{bmatrix} [\mathbf{u}_k]_P & [\mathbf{u}_k]_{P-1} & \cdots & [\mathbf{u}_k]_1 \\ [\mathbf{u}_k]_{P+1} & [\mathbf{u}_k]_P & \cdots & [\mathbf{u}_k]_2 \\ \vdots & \vdots & & \vdots \\ [\mathbf{u}_k]_{M-1} & [\mathbf{u}_k]_{M-2} & \cdots & [\mathbf{u}_k]_{M-P} \end{bmatrix}, \tag{12}$$

$r = -[r_1 \cdots r_P]^T$, $g_k = -[[\mathbf{u}_k]_{P+1} \cdots [\mathbf{u}_k]_M]^T$, and $[\mathbf{u}_k]_M$ is the mth element in u_k.

Table 1: Implementation steps of the proposed algorithm.

(1) An equivalent $\widehat{R}$ is obtained through calculation of formulas (3), (5), (6), (7) and (8)
(2) The Toeplitz matrix containing DOA information is constructed by using formula (10)
(3) Formulas (14)–(16) were combined to obtain formula (18)
(4) Initialize $B(r)$ by using $\widehat{r}_0$ in formula (21), and utilize the $B(r)$ to construct $\widehat{W}$ via formula (18)
(5) The exact $\widehat{r}$ is obtained through several iterations of formulas (18) and (20)
(6) All DOA candidates were obtained by calculating formula (22)
(7) DOA values were obtained from all DOA candidates via formula (23)

Let $\widehat{F}$ and $\widehat{g}$ become estimates of F and g, and then we have the following:

$$\widehat{F}_k r \approx \widehat{g}_k \tag{13}$$

formula (13) cannot be solved directly due to noise. Therefore, the relationship between Toeplitz matrix $B(r)$ and formula (13) should be established. In the case of noise, we find that

$$vec(B(r)U) = vec(B(r)(U_s + \Delta U_s)) = \mathbf{0}_{(M-P)\times k}. \tag{14}$$

By combining formulas (11) and (14), the following can be obtained:

$$vec(B(r)U) = F_k r - g_k = \mathbf{0}_{(M-P)\times k}. \tag{15}$$

2.5. Weighted Least Square Method Used to Solve the Linear Equation. The weighted least square (WLS) method [42] is used to obtain a more accurate estimate, and the cost function is set as follows:

$$(\widehat{e})^H W \widehat{e}, \tag{16}$$

where $W = (\mathrm{E}[\widehat{e}(\widehat{e})^H])^{-1}$, and $\widehat{e} = \widehat{F}r - \widehat{g}$. Then, the solution of formula (16) is as follows:

$$\widehat{r} = \left((\widehat{F})^H W \widehat{F}\right)^{-1} (\widehat{F})^H W \widehat{g}, \tag{17}$$

where we replace r by $\widehat{r}$. However, we cannot obtain the value of $\widehat{r}$ directly, because W is unavailable. Thus, we obtain an estimate of W by combining formulas (14) and (16), as follows:

$$\widehat{W} = \Gamma \otimes \left(B(r)B^H(r)\right)^{-1}, \tag{18}$$

Table 2: Main step complexity of the proposed algorithm.

Main steps	Complexity
$\widehat{R}$	$\mathcal{O}\left(3M^3 + (N+1)M^2\right)$
EVD of $\widehat{R}$	$\mathcal{O}\left(M^3\right)$
$\widehat{W}^{-1}$	$\mathcal{O}\left((M-P)^3\right)$
$\widehat{r}$	$\mathcal{O}\left(2P^2K(M-P) + 2PK(M-P)^2 + P^3 + PK(M-P)\right)$

where W is replaced by $\widehat{W}$, and

$$\widehat{\Gamma} = \begin{bmatrix} \dfrac{\left(\widehat{\lambda}_1 - \widehat{\sigma}_n^2\right)^2}{\lambda_1} & & \\ & \ddots & \\ & & \dfrac{\left(\widehat{\lambda}_K - \widehat{\sigma}_n^2\right)^2}{\widehat{\lambda}_K} \end{bmatrix}, \tag{19}$$

$$\delta^2 = \frac{1}{M-N} \sum_{i=N+1}^{M} \lambda_i.$$

Then, by plugging formula (18) into formula (17), we have the following:

$$\widehat{r} = \left((\widehat{F})^H \widehat{W} \widehat{F}\right)^{-1} (\widehat{F})^H \widehat{W} \widehat{g}.. \tag{20}$$

2.6. Maximum Likelihood Rule Used to Obtain DOA. Multiple $\widehat{r}$ are iteratively obtained, and then the maximum likelihood rule is used

to obtain the exact DOA. First, the initial value of $\widehat{r}$ is obtained by calculation, which can be obtained from formula (13), as follows:

$$\widehat{r}_0 = (\widehat{F})^{\dagger} \widehat{g}, \tag{21}$$

and then formula (21) is substituted into formula (18) to obtain new $\widehat{W}$. The new $\widehat{W}$ is substituted into formula (20) to obtain $\widehat{r}$. After several iterations, we obtain all the DOA candidates as follows:

$$\widehat{\theta}_i = \sin^{-1}\left(\frac{\lambda \angle \widehat{r}_i}{2\pi d}\right), i = 1, \cdots, k. \tag{22}$$

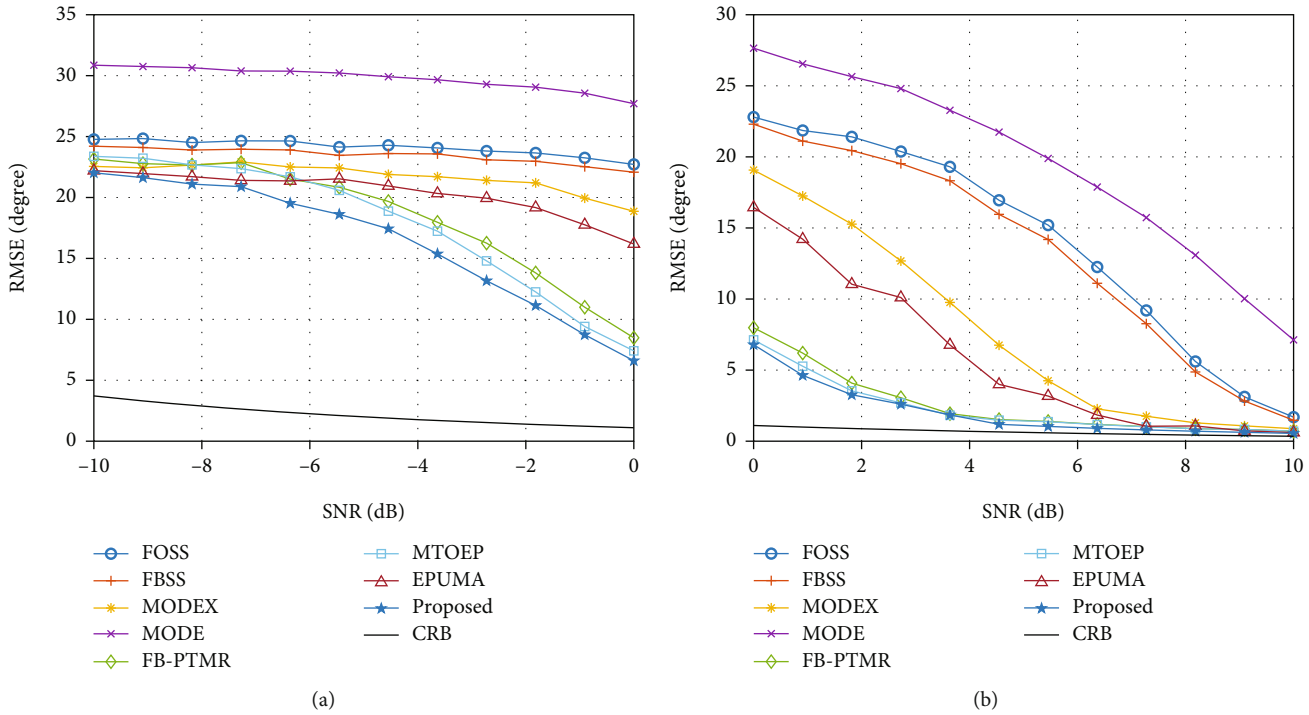

Figure 1: Algorithm RMSE versus *SNR* for two coherent signals and one uncorrelated signal with DOAs being [−5°, 0°, 25°] when $N = 100$. (a) *SNR* increased from −10 dB to 0 dB; (b) *SNR* increased from 0 dB to 10 dB.

Finally, we select estimates from all DOA candidates by maximum likelihood rule, as follows:

$$L(\Theta) = tr\left(\left(I_M - A(\Theta)\left(A^H(\Theta)A(\Theta)\right)^{-1}A^H(\Theta)\right)\widehat{R}\right), \quad (23)$$

where $L(\Theta)$ contains the desired DOA information. The proposed algorithm is summarized in Table 1.

2.7. Complexity Analysis. The main steps of the proposed algorithm are as follows:

(1) Calculation of $\widehat{R}$ and its EVD

(2) Calculation of $\widehat{W}^{-1}$

(3) Calculation of $\hat{r}$

The complexity of the main steps of the proposed algorithm is summarized in Table 2.

The sample covariance matrix and EVD complexity of the proposed algorithm are $\mathcal{O}(3M^3 + (N+1)M^2)$ and $\mathcal{O}(M^3)$, respectively. The computational $\widehat{W}^{-1}$ complexity is mainly caused by $B(r)B^H(r)$, which is about $\mathcal{O}((M-P)^3)$. The complexity of calculating $\hat{r}$ is $\mathcal{O}(2P^2K(M-P) + 2PK(M-P)^2 + P^3 + PK(M-P))$. Finally, the complexity of DOA is obtained by maximum likelihood rule, that is, $\mathcal{O}(G(M^3 + 3MK^2 + K^3))$. Thus, the complexity of the proposed scheme is:

$$\mathcal{O}\left(4M^3 + M^2(N+1) + I\left(M^3 - K^3 - 11MK^2 - 2M^2K + 4K^3M + 4K^2M^2\right) + G\left(M^3 + 3MK^2 + K^3\right)\right), \quad (24)$$

where I is the number of iterations, and $G = (P+K)!/K!P!$. Due to $G \gg I$ and isotropic sensors $M \gg K$, the complexity is reduced to $\mathcal{O}((N+1)M + GM^3)$.

3. Results and Discussion

In this section, we present a series of experiments to verify the superior performance of the proposed algorithm and consider ESPRIT [14], MODE [27], MODEX [31], EPUMA [29], FB-PTMR [35], and MTOEP [40] for comparison. The Cramér–Rao Bound (CRB) is used as a measure of performance in the experiment. In addition, FBSS [21] and FOSS [22] technologies are used to improve the ability of ESPRIT to process coherent signals. During the experiment, we assume that all signals are narrowband signals, and the ULA composed of $M = 10$ sensors is used to receive K signals. In order to demonstrate the advantage of the proposed algorithm in dealing with coherent signals, in the following experiments, coherence coefficient is 1. Furthermore, 3000 Monte Carlo experiments are performed for each experiment to obtain more accurate experimental data. The root mean square error (RMSE) of DOA is as follows:

$$\text{RMSE} = \sqrt{\frac{1}{3000K}\sum_{k=1}^{K}\sum_{i=1}^{3000}\left(\widehat{\theta}_{k,i} - \theta_k\right)^2}, \quad (25)$$

where $\widehat{\theta}_{k,i}$ is the experimental value and θ_k is the true value.

In the first experiment, we study the effect of different *SNR* on the RMSE and resolution of the algorithm. Three signals with DOAs being [−5°, 0°, 25°]are consider (K=3),

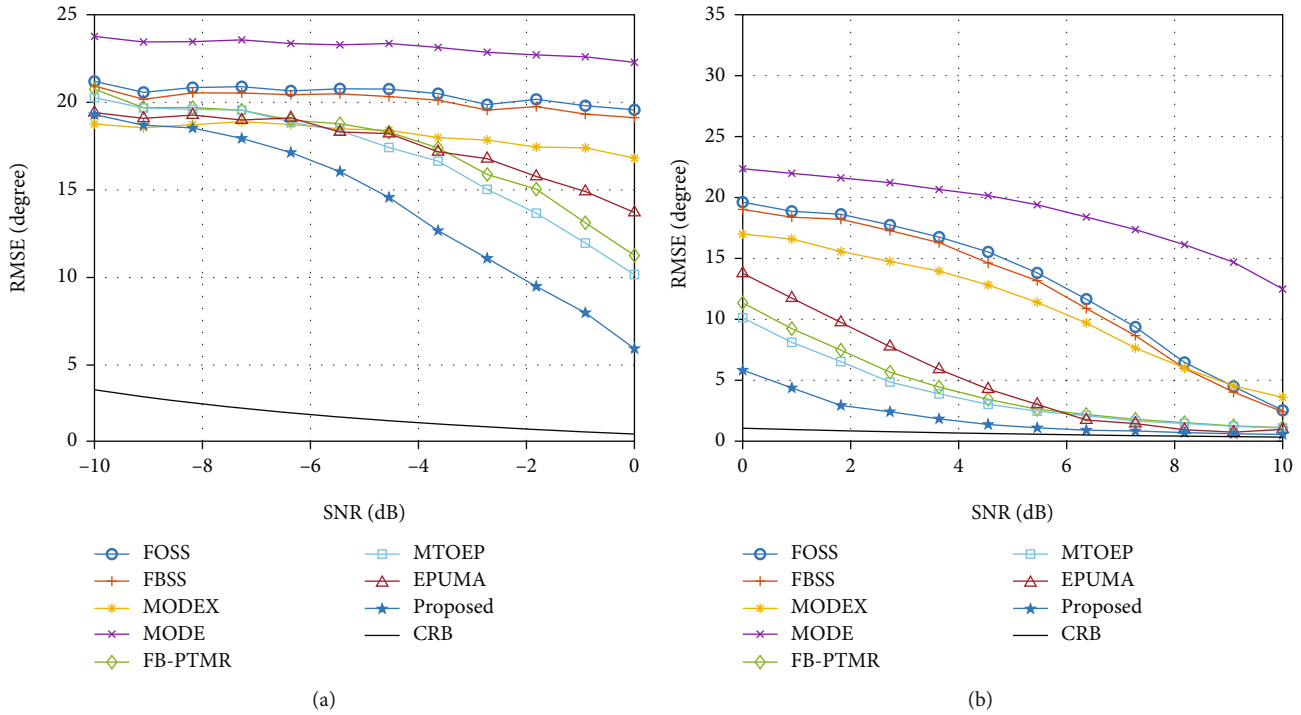

Figure 2: Algorithm RMSE versus *SNR* for two coherent signals and two uncorrelated signals with DOAs being [−5°, 0°, 25°, 31°] when $N = 100$. (a) *SNR* increased from −10 dB to 0 dB; (b) *SNR* increased from 0 dB to 10 dB.

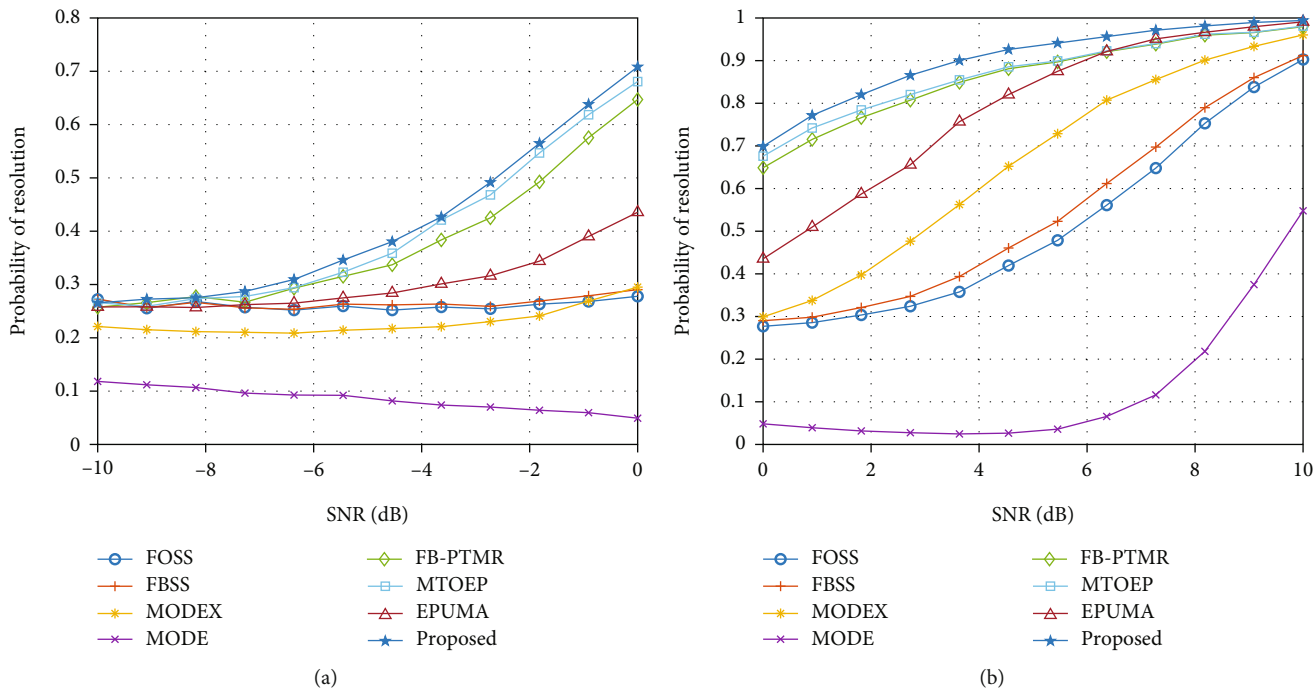

Figure 3: Algorithm probability versus *SNR* for two coherent signals and two uncorrelated signals with DOAs being [−5°, 0°, 25°] when $N = 100$. (a) *SNR* increased from −10 dB to 0 dB; (b) *SNR* increased from 0 dB to 10 dB.

where the first two signals are coherent and uncorrelated with the third one. We can obtain RMSE from (25), and the snapshot number is $N = 100$. As shown in Figure 1, when $SNR < 0$ dB, the RMSE of all algorithms are far from the CRB, FB-PTMR, and MTOEP, and the proposed algorithms are slightly better than the other algorithms. When $SNR > 0$ dB and $K = 3$, the RMSE of all algorithms is reduced, as well as the FB-PTMR, MTOEP, and the proposed converge to the

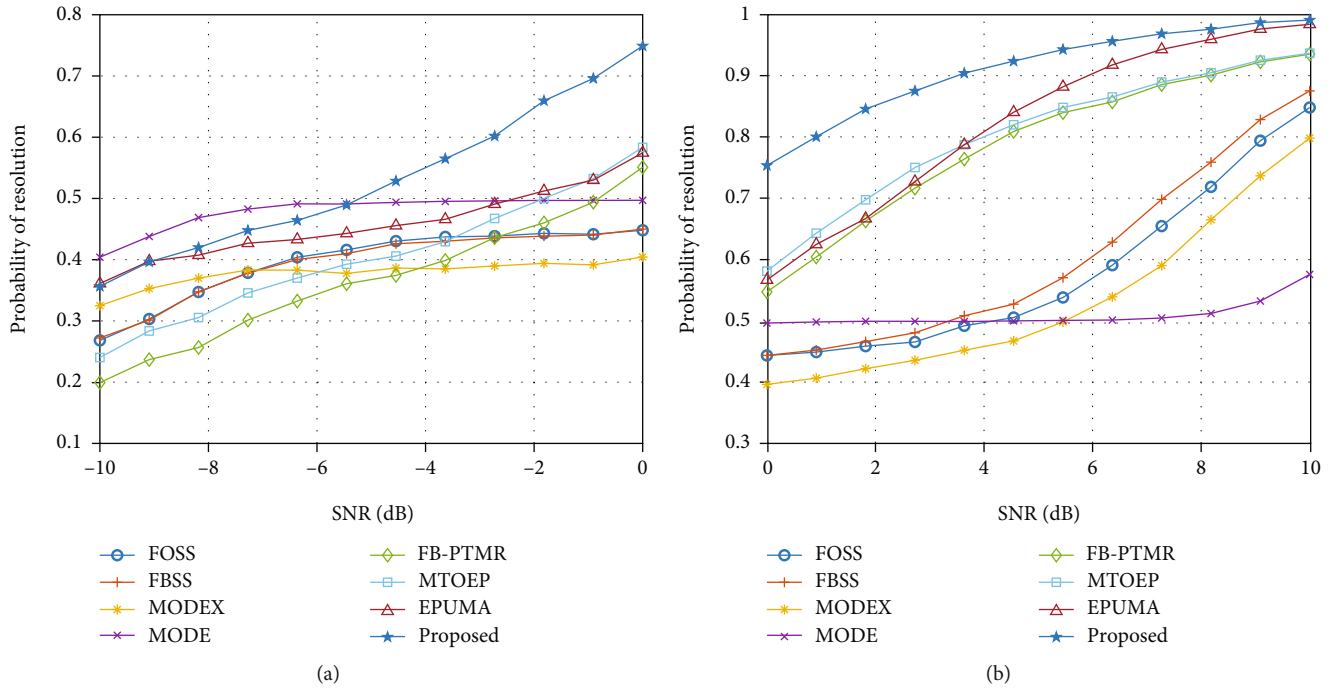

Figure 4: Algorithm probability versus *SNR* for two coherent signals and two uncorrelated signals with DOAs being [−5°, 0°, 25°, 31°] when $N = 100$. (a) *SNR* increased from −10 dB to 0 dB; (b) *SNR* increased from 0 dB to 10 dB.

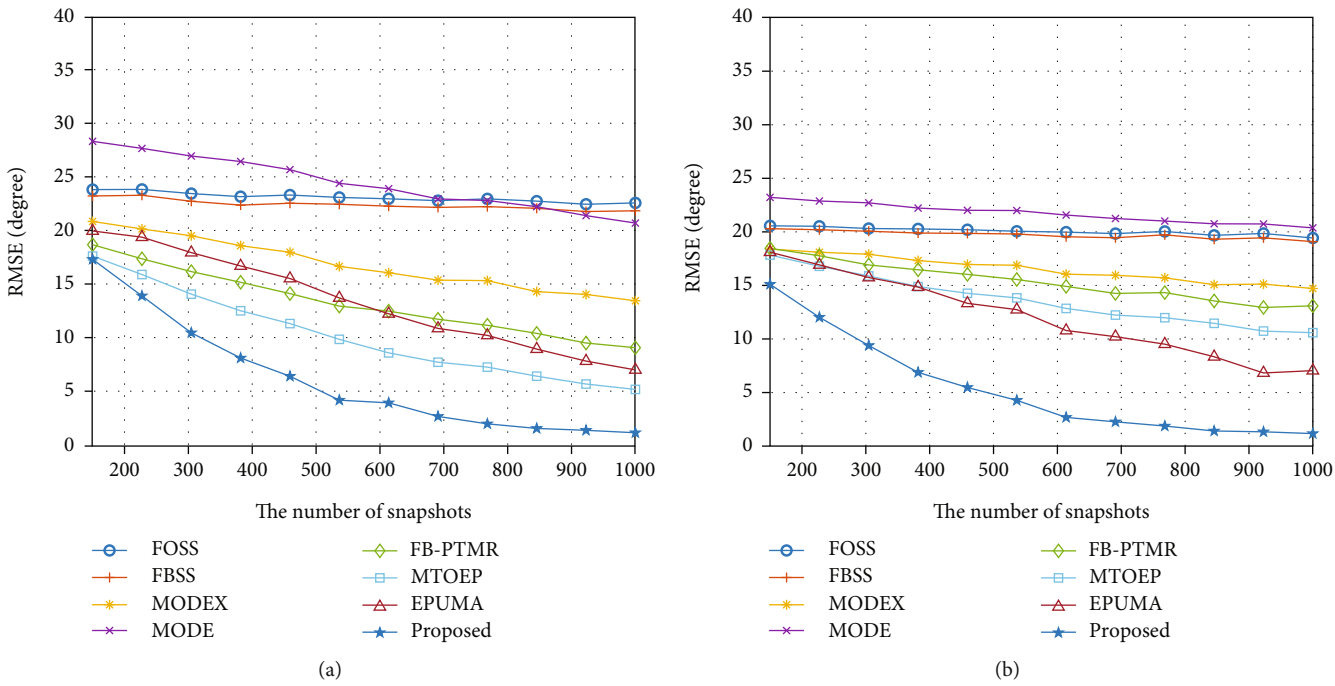

Figure 5: Algorithm RMSE versus snapshot number when $SNR = -5$ dB. (a) Two coherent signals and one uncorrelated signals with DOAs being [−5°, 0°, 25°]; (b) two coherent signals and two uncorrelated signals with DOAs being [−5°, 0°, 25°, 31°].

CRB when $SNR = 5$ dB. Meanwhile, due to the lack of array aperture, although ESPRIT optimized by FOSS and FBSS can process coherent signals, the RMSE of the optimized ESPRIT does not completely converge to the CRB until *SNR* = 10 dB. The performance is the best when using EPUMA and MODEX on $SNR > 6$ dB, MODE always has a large distance from the CRB, and its ability to process coherent signals is poor.

To further verify the performance of the proposed algorithm, an uncorrelated signal ($K = 4$) is added. Figure 2

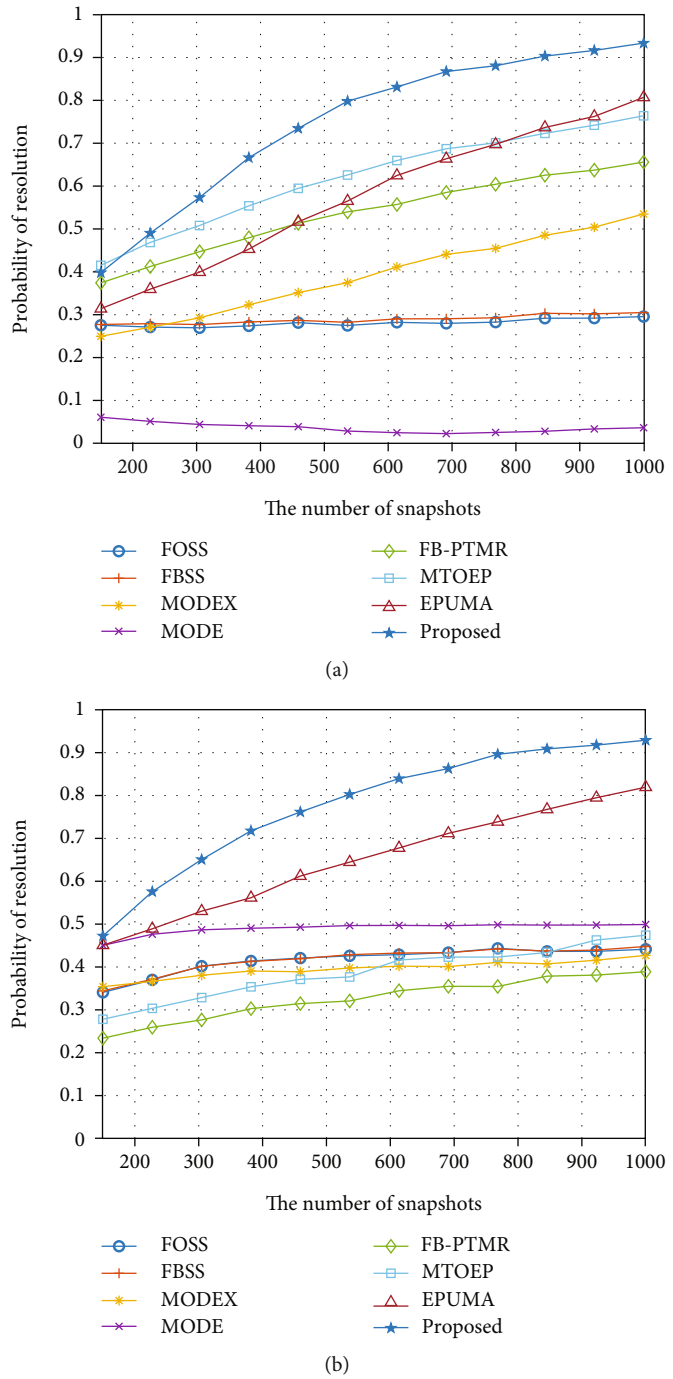

Figure 6: Algorithm probability versus snapshot number when $SNR = -5$ dB. (a) Two coherent signals and one uncorrelated signals with DOAs being $[-5^\circ, 0^\circ, 25^\circ]$; (b) two coherent signals and two uncorrelated signals with DOAs being $[-5^\circ, 0^\circ, 25^\circ, 31^\circ]$.

shows that, similar to $K = 3$, when $SNR < 0$ dB, the RMSE of all algorithms is large and far from the CRB. The RMSE of the proposed algorithm is smaller than that of other algorithms. When $SNR = 6$ dB and $SNR > 8$ dB, the proposed algorithm and EPUMA converge to the CRB, respectively. FB-PTMR and MTOEP still have a gap with the CRB even when $SNR = 10$ dB. Compared with $K = 3$, when $K = 4$, only the proposed algorithm is unaffected by the number of signals, whereas the other algorithms are affected by the number of signals, among which MODEX is the most affected.

The influence of SNR on algorithm resolution is shown in Figures 3 and 4. When $K = 3$, $SNR<0$ dB, the resolution of FB-PTMR, MTOEP, and the proposed algorithm is lower than 80%, whereas other algorithms are lower than 50%. With the increase in SNR, the resolution of all algorithms increases rapidly. Except for MODE, when $SNR = 10$ dB, the performance reached or exceeded 90%. When $K = 4$, $SNR < 0$ dB, the resolution of the proposed algorithm is much higher than that of the other algorithms but lower than 80%. When $SNR = 10$ dB, only the resolution of EPUMA,

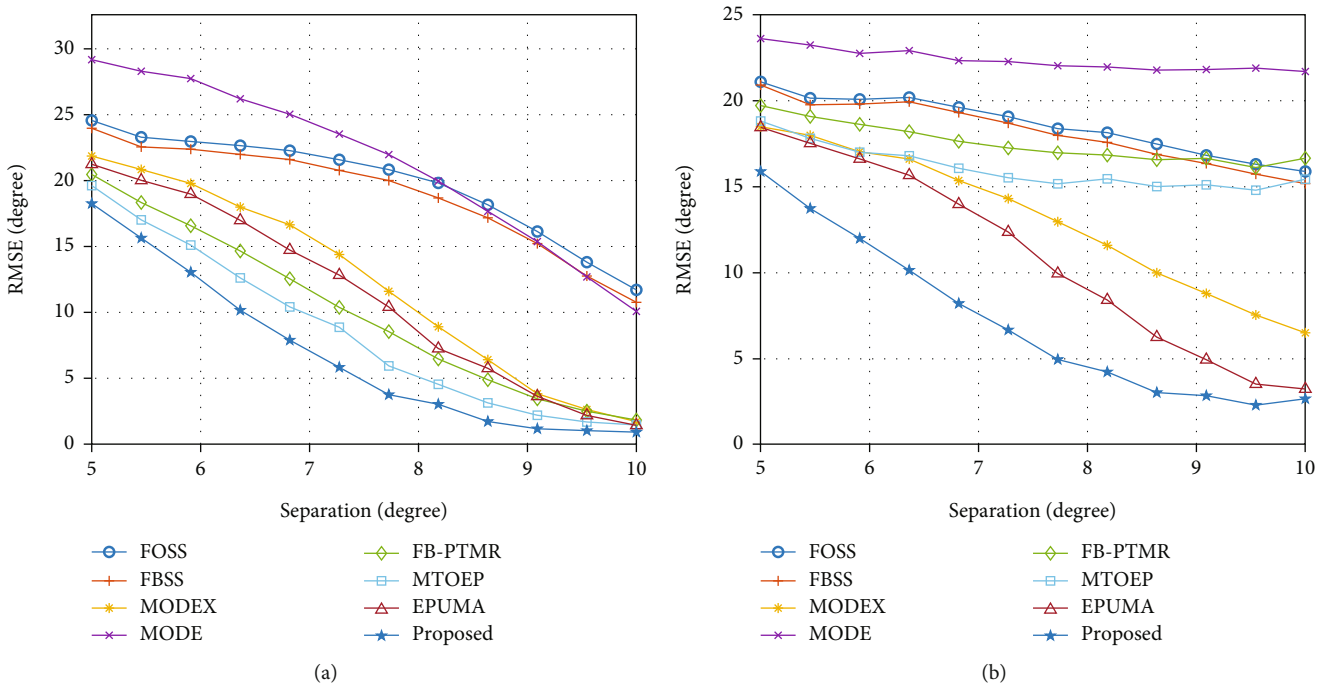

Figure 7: Algorithm RMSE versus $\Delta\theta$ when $SNR = -5$ dB. (a) Two coherent signals and one uncorrelated signal with DOAs being $[-5^\circ, 0^\circ + \Delta\theta, 25^\circ]$; (b) two coherent signals and two uncorrelated signals with DOAs being $[-5^\circ, 0^\circ + \Delta\theta, 25^\circ, 31^\circ]$.

MTOEP, FB-PTMR, and the proposed algorithm reaches or even exceeds 90%, whereas that of the other algorithms is lower than 90%.

This group of experiments verifies that the proposed algorithm has good anti-interference ability and can still effectively process coherent signals when facing multiple signals and different *SNR*, with small error and high resolution, which is unavailable in other algorithms. Under certain conditions, the resolution of the proposed algorithm even reaches 95%, whereas that of other algorithms is greatly affected by the number of signals. In addition, the error increases evidently, and the resolution decreases when processing multiple signals. Furthermore, this group of experiments show the advantage of the proposed algorithm in processing coherent signals at low *SNR*, and the next experiments will further study the ability of the proposed algorithm to handle coherent signals in different situations when $SNR = -5$ dB.

In the second experiment, we study the effect of different snapshot numbers on the RMSE and resolution of the algorithm. The experimental conditions are the same as the first experiment. Figure 5 shows that the performance of the proposed algorithm is better than that of the other algorithms. When $K = 3$, with the increase in snapshot number, the proposed algorithm converges rapidly, and RMSE decreases. Although the RMSE of MODEX, FB-PTMR, MTOEP, and EPUMA is also reduced, it is not as good as the proposed algorithm. However, FOSS, FBSS, and MODE almost remain unchanged, and their errors are much higher than those of the other algorithms, even if the snapshot number is 1000. When $K = 4$, the proposed algorithm still has better processing ability and is unaffected by the number of signals. EPUMA is less affected by the number of affected signals, and RMSE is basically unchanged, but not as good as the proposed algorithm. However, the other algorithms are greatly affected by the number of signals, and the RMSE increases.

Figure 6 shows that when $K = 3$, the resolution of EPUMA and MTOEP can be close to or reaches 80%, whereas when $K = 4$, the resolution of MTOEP decreases seriously and is lower than 50%. Other algorithms have low resolution in any case, but the proposed algorithm can still have a resolution higher than 90% under any condition.

Therefore, compared with other algorithms, the proposed algorithm can effectively use snapshot to detect signal information, and the estimation accuracy is high. It can process multiple signals with a high resolution of more than 90%, whereas other algorithms are inferior to the proposed algorithm with a low resolution.

In the third experiment, we study the effect of different angular separation on the RMSE and resolution of the algorithm. The parameters remained the same as in the first experiment. In Figure 7, when $K = 3$ and separation is 9, the MTOEP and the proposed algorithm reach the optimal state. In addition, the other algorithms are not at their best even when the separation is 10. When $K = 4$, only EPUMA and the proposed algorithm are less affected by the number of signals, with RMSE decreasing significantly as separation increases, whereas the RMSE of the other algorithms decreases but not as much as EPUMA and the proposed algorithm.

As in the previous experiment, we also tested the angular separation impact on algorithm resolution. As shown in Figure 8, when $K = 3$, the resolution of EPUMA and the

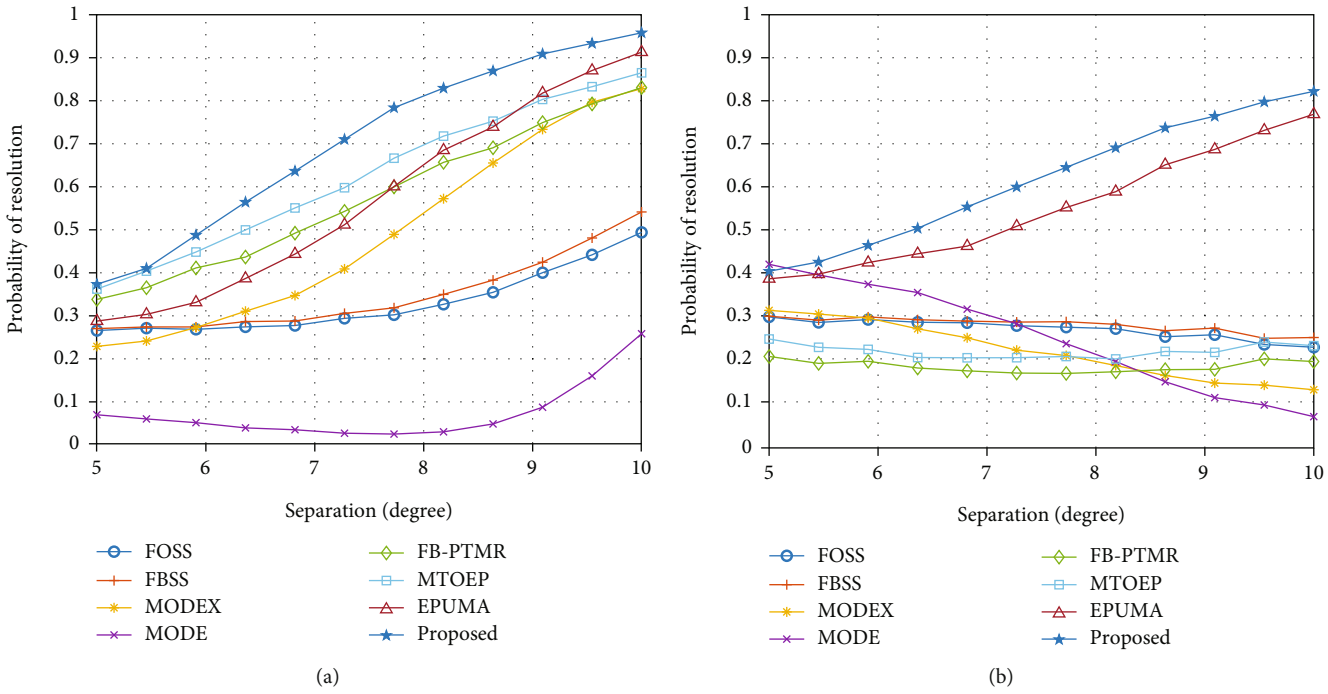

FIGURE 8: Algorithm probability versus $\Delta\theta$ when $SNR = -5$ dB. (a) Two coherent signals and one uncorrelated signals with DOAs being $[-5^\circ, 0^\circ + \Delta\theta, 25^\circ]$; (b) two coherent signals and two uncorrelated signals with DOAs being $[-5^\circ, 0^\circ + \Delta\theta, 25^\circ, 31^\circ]$.

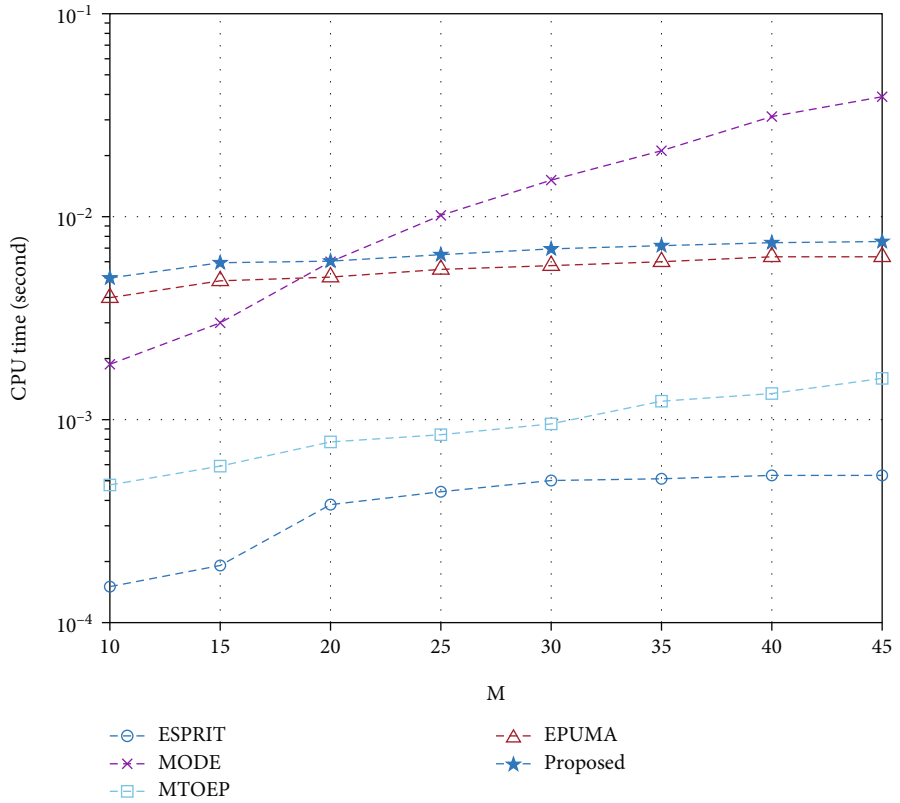

FIGURE 9: CPU time versus M when $K = 3$ and $N = 80$.

proposed algorithm reaches or even exceeds 90%. The resolution of MTOEP, FB-PTMR, and MODEX also exceeds 80%, and that of the remaining algorithms does not exceed 60%. When $K = 4$, the resolution of all algorithms decreases seriously. The performance of EPUMA and the proposed algorithm is reduced from 90% to about 80%,

whereas that of other algorithms is lower than or equal to 30%.

This set of experiments demonstrates that the proposed algorithm is relatively affected when dealing with angular separation variations of multiple coherent signals ($K = 4$), but the resolution is still higher than that of the other algorithms under the same conditions; the resolution of the algorithm reaches 80%. When the number of signals is small ($K = 3$), the resolution of the proposed algorithm can still exceed 90%. The performance of other algorithms is far inferior to that of the proposed algorithm.

Finally, because FB-PTMR, FBSS, and FOSS are all based on ESPRIT algorithm, MODEX complexity is extremely huge, so we compare the complexity of ESPRIT, MODE, MTOEP, EPUMA, and the proposed algorithm. We assume that three signals are available, N is 80, and we vary M from 10 to 45. Through calculation, we obtain that the complexity of ESPRIT, MODE, MTOEP, and EPUMA is $\mathcal{O}(M^2N + M^3)$, $\mathcal{O}((8K^3 + 1)(M - K)^3)$, $\mathcal{O}(4M^3 + (N + 1)M^2)$, and $\mathcal{O}(M^2N + GM^3)$, respectively. Figure 9 shows that ESPRIT has simple computational complexity, whereas the standard MODE is the most computationally intensive method among the six competitors. The computational complexity of the proposed algorithm and EPUMA is similar.

4. Conclusions

An efficient algorithm without auxiliary matrix and noise preprocessing is proposed by combining the advantages of polynomial solving DOA signal and Toeplitz matrix reconstruction. In the face of multiple signals, the performance of other reference algorithms has been greatly affected, whereas the proposed algorithm still has high estimation accuracy. Simulation experiments show that the proposed algorithm has the advantage of processing multiple signals containing coherent signals, and it is less affected by *SNR* and snapshot number, which is an advantage that other reference algorithms do not have. Under certain conditions, the resolution can reach 90% and sometimes exceed 95%. Although the proposed algorithm has many advantages, when angular separation changes and with multiple signals ($K = 4$), the proposed algorithm is affected to some extent, and the resolution is only 80%. However, when $K = 3$, the resolution immediately increases to 95%. In addition, the proposed algorithm has low complexity. This paper provides a signal location method with high estimation accuracy, strong anti-interference ability, and effective processing of multiple signals.

Data Availability

Data are only available upon request due to restrictions regarding, e.g., privacy and ethics. The data presented in this study are available from the corresponding author upon request. The data are not publicly available due to their relation to other ongoing research.

Conflicts of Interest

The authors declare no conflict of interest.

Acknowledgments

This work was supported by the National Natural Science Foundation of China (No. 61763018), the Central Guided Local Science and Technology Funding Project of the Science and Technology Department of Jiangxi Province (Cross-regional Cooperation, 20221ZDH04052), the 03 Special Project and 5G Program of the Science and Technology Department of Jiangxi Province (No. 20193ABC03A058), the China Scholarship Council (CSC, No. 201708360150), the Key Foundation of Education Committee of Jiangxi (Nos. GJJ170493 and GJJ190451), the Program of Qingjiang Excellent Young Talents in Jiangxi University of Science and Technology (JXUSTQJBJ2019004), and the Cultivation Project of the State Key Laboratory of Green Development and High-Value Utilization of Ionic Rare-Earth Resources in Jiangxi Province (20194AFD44003), the Key Research and Development Plan of Ganzhou (industrial field), and the Science and Technology Innovation Talent Project of Ganzhou.

References

[1] A. Norrdine, H. Cetinkaya, and R. Herschel, "Radar wave based positioning of spatially distributed MIMO radar antenna systems for near-field nondestructive testing," *IEEE Sensors Letters*, vol. 4, no. 5, pp. 1–4, 2020.

[2] S. G. Dontamsetti and R. V. R. Kumar, "A distributed MIMO radar with joint optimal transmit and receive signal combining," *IEEE Transactions on Aerospace and Electronic Systems*, vol. 57, no. 1, pp. 623–635, 2021.

[3] X.-h. Sheng and H. Yu-Hen, "Maximum likelihood multiple-source localization using acoustic energy measurements with wireless sensor networks," *IEEE Transactions on Signal Processing*, vol. 53, no. 1, pp. 44–53, 2005.

[4] I. Bekkerman and J. Tabrikian, "Target detection and localization using MIMO radars and sonars," *IEEE Transactions on Signal Processing*, vol. 54, no. 10, pp. 3873–3883, 2006.

[5] X. Chao, C. Fan, and X. Huang, "Time reversal linearly constrained minimum power algorithm for direction of arrival estimation in diffuse multipath environments," *Remote Sensing*, vol. 12, no. 20, p. 3344, 2020.

[6] J. W. Paik, W. Hong, and J.-H. Lee, "Direction-of-Departure and direction-of-arrival estimation algorithm based on compressive sensing: data fitting," *Remote Sensing*, vol. 12, no. 17, p. 2773, 2020.

[7] Y. Quan, R. Zhang, Y. Li, R. Xu, S. Zhu, and M. Xing, "Microwave correlation forward-looking super-resolution imaging based on compressed sensing," *IEEE Transactions on Geoscience and Remote Sensing*, vol. 59, no. 10, pp. 8326–8337, 2021.

[8] H. Zhang, J. Shi, Q. Zhang, B. Zong, and J. Xie, "Antenna selection for target tracking in collocated MIMO radar," *IEEE Transactions on Aerospace and Electronic Systems*, vol. 57, no. 1, pp. 423–436, 2021.

[9] Y. Qian, Z. Yang, and H. Zeng, "Direct position determination for augmented coprime arrays via weighted subspace data fusion method," *Mathematical Problems in Engineering*, vol. 2021, Article ID 2825025, 10 pages, 2021.

[10] K. N. R. S. V. Prasad, E. Hossain, and V. K. Bhargava, "Energy efficiency in massive MIMO-based 5G networks: opportunities and challenges," *IEEE Wireless Communications*, vol. 24, no. 3, pp. 86–94, 2017.

[11] L. Liu and H. Liu, "Joint estimation of DOA and TDOA of multiple reflections in mobile communications," *IEEE Access*, vol. 4, pp. 3815–3823, 2016.

[12] R. Shafin, L. Liu, J. Zhang, and Y. C. Wu, "DoA estimation and capacity analysis for 3-D millimeter wave massive-MIMO/FD-MIMO OFDM systems," *IEEE Transactions on Wireless Communications*, vol. 15, no. 10, pp. 6963–6978, 2016.

[13] R. Schmidt, "Multiple emitter location and signal parameter estimation," *IEEE Transactions on Antennas and Propagation*, vol. 34, no. 3, pp. 276–280, 1986.

[14] T. Kailath, "ESPRIT–estimation of signal parameters via rotational invariance techniques," *Optical Engineering*, vol. 29, no. 4, p. 296, 1990.

[15] B.-s. Kim, Y. Jin, J. Lee, and S. Kim, "Low-complexity MUSIC-based direction-of-arrival detection algorithm for frequency-modulated continuous-wave vital radar," *Sensors*, vol. 20, no. 15, p. 4295, 2020.

[16] E. D. D. Claudio, R. Parisi, G. Jacovitti, and G. Jacovitti, "Space time MUSIC: consistent signal subspace estimation for wide-band sensor arrays," *IEEE Transactions on Signal Processing*, vol. 66, no. 10, pp. 2685–2699, 2018.

[17] M. Wagner, Y. Park, and P. Gerstoft, "Gridless DOA estimation and root-MUSIC for non-uniform linear arrays," *IEEE Transactions on Signal Processing*, vol. 69, pp. 2144–2157, 2021.

[18] T. T. Zhang, H. T. Hui, and Y. Lu, "Compensation for the mutual coupling effect in the ESPRIT direction finding algorithm by using a more effective method," *IEEE Transactions on Antennas and Propagation*, vol. 53, no. 4, pp. 1552–1555, 2005.

[19] J. Steinwandt, F. Roemer, and M. Haardt, "Generalized least squares for ESPRIT-type direction of arrival estimation," *IEEE Signal Processing Letters*, vol. 24, no. 11, pp. 1681–1685, 2017.

[20] J. Pan, M. Sun, Y. Wang, and X. Zhang, "An enhanced spatial smoothing technique with ESPRIT algorithm for direction of arrival estimation in coherent scenarios," *IEEE Transactions on Signal Processing*, vol. 68, pp. 3635–3643, 2020.

[21] T. J. Shan, M. Wax, and T. Kailath, "On spatial smoothing for direction-of-arrival estimation of coherent signals," *IEEE Transactions on Acoustics, Speech, and Signal Processing*, vol. 33, no. 4, pp. 806–811, 1985.

[22] S. Pillai and B. Kwon, "Forward/backward spatial smoothing techniques for coherent signal identification," *IEEE Transactions on Acoustics, Speech, and Signal Processing*, vol. 37, no. 1, pp. 8–15, 1989.

[23] M. Viberg and B. Ottersten, "Sensor array processing based on subspace fitting," *IEEE Transactions on Signal Processing*, vol. 39, no. 5, pp. 1110–1121, 1991.

[24] P. Stoica, B. Ottersten, M. Viberg, and R. Moses, "Maximum likelihood array processing for stochastic coherent sources," *IEEE Transactions on Signal Processing*, vol. 44, no. 1, pp. 96–105, 1996.

[25] J. Sheinvald, M. Wax, and A. J. Weiss, "On maximum-likelihood localization of coherent signals," *IEEE Transactions on Signal Processing*, vol. 44, no. 10, pp. 2475–2482, 1996.

[26] Y. H. Choi, "Maximum likelihood estimation for angles of arrival of coherent signals using a coherency profile," *IEEE Transactions on Signal Processing*, vol. 48, no. 9, pp. 2679–2682, 2000.

[27] A. B. Gershman and P. Stoica, "New MODE-based techniques for direction finding with an improved threshold performance," *Signal Processing*, vol. 76, no. 3, pp. 221–235, 1999.

[28] P. Stoica and K. Sharman, "Novel eigenanalysis method for direction estimation," *IEE Proceedings F Radar and Signal Processing*, vol. 137, no. 1, pp. 19–26, 1990.

[29] C. Qian, L. Huang, N. D. Sidiropoulos, and H. C. So, "Enhanced PUMA for direction-of-arrival estimation and its performance analysis," *IEEE Transactions on Signal Processing*, vol. 64, no. 16, pp. 4127–4137, 2016.

[30] P. Stoica and M. Jansson, "On forward–backward MODE for array signal processing," *Digital Signal Processing*, vol. 7, no. 4, pp. 239–252, 1997.

[31] A. Gershman and P. Stoica, "MODE with extra-roots (MODEX): a new DOA estimation algorithm with an improved threshold performance," in *1999 IEEE International Conference on Acoustics, Speech, and Signal Processing. Proceedings. ICASSP99 (Cat. No.99CH36258)*, vol. 5, pp. 2833–2836, Phoenix, AZ, USA, 1999.

[32] F. Wen and H. C. So, "Tensor-MODE for multi-dimensional harmonic retrieval with coherent sources," *Signal Processing*, vol. 108, pp. 530–534, 2015.

[33] C. Qian, L. Huang, M. Cao, J. Xie, and H. C. So, "PUMA: an improved realization of MODE for DOA estimation," *IEEE Transactions on Aerospace and Electronic Systems*, vol. 53, no. 5, pp. 2128–2139, 2017.

[34] S. Liu, Z. Mao, Y. D. Zhang, and Y. Huang, "Rank minimization-based Toeplitz reconstruction for DoA estimation using coprime array," *IEEE Communications Letters*, vol. 25, no. 7, pp. 2265–2269, 2021.

[35] W. Zhang, Y. Han, M. Jin, and X. S. Li, "An improved ESPRIT-like algorithm for coherent signals DOA estimation," *IEEE Communications Letters*, vol. 24, no. 2, pp. 339–343, 2020.

[36] C. Qian, L. Huang, W. J. Zeng, and H. C. So, "Direction-of-arrival estimation for coherent signals without knowledge of source number," *IEEE Sensors Journal*, vol. 14, no. 9, pp. 3267–3273, 2014.

[37] Y. Zhang, S. Liu, Z. Mao, and Y. Huang, "DoA estimation based on accelerated structured alternating projection using coprime array," in *Seventh Asia Pacific Conference on Optics Manufacture (APCOM 2021)*, pp. 1–9, Hong Kong, 2021.

[38] J. Dai and H. C. So, "Real-valued sparse Bayesian learning for DOA estimation with arbitrary linear arrays," *IEEE Transactions on Signal Processing*, vol. 69, pp. 4977–4990, 2021.

[39] B. Cai, Y.-M. Li, and H. Y. Wang, "Forward/backward spatial reconstruction method for directions of arrival estimation of uncorrelated and coherent signals," *IET Microwaves, Antennas and Propagation*, vol. 6, no. 13, pp. 1498–1505, 2012.

[40] W. Zhang, Y. Han, M. Jin, and X. Qiao, "Multiple-Toeplitz matrices reconstruction algorithm for DOA estimation of coherent signals," *IEEE Access*, vol. 7, pp. 49504–49512, 2019.

[41] Y. Chan, J. Lavoie, and J. Plant, "A parameter estimation approach to estimation of frequencies of sinusoids," *IEEE Transactions on Acoustics, Speech, and Signal Processing*, vol. 29, no. 2, pp. 214–219, 1981.

[42] E. GrosicKi, K. Abed-Meraim, and Y. Hua, "A weighted linear prediction method for near-field source localization," *IEEE Transactions on Signal Processing*, vol. 53, no. 10, pp. 3651–3660, 2005.